Conduction processes in the layered semiconductor compound $FePS_3$

V. Grasso, F. Neri, S. Patanè, and L. Silipigni
Istituto di Struttura della Materia, Università degli Studi di Messina, Salita Sperone 31, P.O. Box 57, I-98166 S. Agata Messina, Italy

M. Piacentini
Dipartimento di Energetica, Università degli Studi di Roma I, "La Sapienza," I-00185 Roma, Italy
(Received 4 December 1989; revised manuscript received 22 February 1990)

We have measured, as a function of temperature, the thermopower, the dc conductivity, and photoconductivity of $FePS_3$ single crystals. For temperatures below 430 K the thermopower shows an activated behavior, whereas at higher temperatures it is almost temperature independent. The dc dark conductivity and photoconductivity are thermally activated over the entire investigated temperature range. Moreover, ac-conductivity measurements have been carried out as a function of both temperature and frequency from 400 Hz to 100 kHz in the 340–500-K temperature region. The transport mechanisms involved in different temperature ranges have been identified. The results have been interpreted on the basis of a simplified energy-band scheme.

INTRODUCTION

The layered compound $FePS_3$ has received considerable attention in recent years for its potential use as cathode material in lithium-anode secondary batteries[1–4] and for its magnetic properties.[5,6]

The synthesis of pure $FePS_3$ is a complicated task because of the large quantities of unreacted phase (seemingly sulfur) remaining in the reaction tubes.[2,3,7] This could explain the observed nonstoichiometry since lamellar compounds, such as $FePS_3$, could accommodate a metal excess in the van der Waals gap.[8] Thompson and Whittingham reported that their $FePS_3$ samples were metal-rich,[2] while Foot *et al.* observed a slight deficiency of iron, up to about 0.1%, which in their opinion was more in keeping with a supposed *p*-type semiconduction.[9]

While the electrical transport properties of $NiPS_3$ and $MnPS_3$ have been studied and satisfactorily interpreted,[10,11] no systematic study of these properties has been yet performed for pure $FePS_3$. Therefore, we have investigated the temperature dependence of the $FePS_3$ conduction mechanism by means of intralayer dc dark conductivity and photoconductivity and thermopower measurements as a function of the temperature. The experimental results indicate that $FePS_3$ is a semiconductor, and they give clear evidence of the carrier type. The thermally activated behavior has allowed us to derive more detailed information on the distribution of the electronic density of states in the energy-gap region. We have also proposed a scheme for the conduction process consistent with the transition-metal weakly interacting model[12] and the obtained experimental values.

We have also analyzed the temperature and frequency dependence of the $FePS_3$ ac conductivity. The experimental results support the conclusions drawn for dc measurements and provide further information about the electrical transport processes taking place near the Fermi level.

EXPERIMENT

In a cryostat operating from liquid-N_2 temperature up to about 500 K, we have carried out extensive studies of thermopower, in-layer conductivity, both dc and ac, and photoconductivity measurements on a single crystal of $FePS_3$ compound $0.5\times3\times4.6$ mm^3 in size. Such samples, grown and supplied by Professor R. Brec of the University of Nantes (France), are black, flexible, and hexagonal plates. During the measurements the pressure was maintained at about 10^{-6} Torr. All measurements were repeated several times on two samples of about equal dimensions in order to check their reproducibility. In particular, the reproducibility for the dark conductivity and photoconductivity measurements was better than 13%. Before each experimental run, the specimen was heated up to 470 K in a vacuum of $\sim10^{-6}$ Torr to avoid the formation of free surface adsorbates. In order to collect all data and to calculate the conductivity, photoconductivity, and thermopower values in real time, a HP3421A data logger, connected to a microcomputer, was used. The dc dark conductivity and photoconductivity measurements were made at heating rates less than 1 °C/min to avoid undesired effects due to thermostimulated currents. The polarization voltage (about 1 V) was provided by a HP 6115 Å precision voltage supply, while the current was measured by a Keithley model 616 electrometer with 10^{14} Ω input impedance. Photoconductivity was excited by a 75-W xenon arc lamp with a measured light intensity of about 500 mW cm^{-2}. The bandwidth of the incident radiation was determined by a visible transmitting filter. In the Seebeck coefficient measurements, the differential method, described in a previous paper,[10] was adopted. The in-layer ac-conductivity measurements were per-

formed from 400 Hz to 100 kHz in the 340–500-K temperature range, using both a phase detection technique with a digital lock-in amplifier and a GenRad 1689M Precision RLC Digibridge.

RESULTS

The thermopower S of $FePS_3$ as a function of reciprocal temperature is shown in Fig. 1. The most remarkable feature of this plot is the change of the thermopower sign from positive at temperatures below 430 K to negative at higher temperatures. In the region where S is positive the data seem to be almost linear in 1000/T. The positive sign of S and the increase of its magnitude with decreasing temperature indicate that $FePS_3$ behaves as a p-type semiconductor in this temperature range. For temperatures above 430 K the plot shows an almost temperature-independent and negative thermopower. The negative sign of S shows that in this temperature region electrons dominate the electrical transport in this compound.

The temperature range, over which the thermopower experimental data were collected, was limited by the high sample resistance at the lowest temperature (this is the reason for the relatively large error bars in region I of Fig. 1) and by the thermal losses which cause a limit to the sample holder thermal equilibrium at the highest ones.

For temperatures below 430 K, where S is thermally activated, the experimental data were fitted to the following formula:

$$S=(k/q)(E_s/kT+A)\ , \tag{1}$$

where k is the Boltzmann's constant, q denotes the charge carrier, E_s measures the energy difference between the Fermi-level energy and the energy of the level where the charge transport occurs, and AkT is the average energy of the transported charge carriers, measured with respect to the energy of the valence-band edge. The value of A depends on the nature of the scattering process. Such a fit, calculated with a weighted least-squares algorithm, which takes into account the uncertainties affecting S,[13] is represented by the dashed line in Fig. 1. The estimated values of E_s and S_0, where $S_0=kA/q$, are (0.52 ± 0.07) eV and (-1.21 ± 0.18) mV K^{-1}, respectively.

Figure 2 shows the temperature dependence of both the $FePS_3$ dark conductivity σ_d and photoconductivity σ_{ph}. The latter was obtained using a visible transmitting filter (photon energies ranging from 1.75 to 4.3 eV). Each curve represents an average over several different experimental runs performed at heating rate less than 1 °C/min. On switching off the light, the photoconductivity reverts to its dark value almost instantaneously. For temperatures below 430 K both curves exhibit an activated behavior, which can be properly approximated by the following formula:

$$\sigma=\sigma_0\exp(-E_a/kT)\ , \tag{2}$$

where E_a is the activation energy and σ_0 indicates the preexponential factor. In Table I the obtained σ_0 and E_a values are reported.

In Figs. 3(a) and 3(b), the $FePS_3$ ac conductivity, σ_{ac}, from 400 Hz to 100 kHz and in 340–500 K temperature range is shown. At temperatures below 400 K the conductivity exhibits a significant frequency dependence. At the highest frequencies the ac conductivity appears to be almost linearly dependent on frequency following an ω^s behavior with $s\simeq0.89$. As temperature is raised, the conductivity becomes less frequency dependent and a progressively stronger temperature dependence is observed.

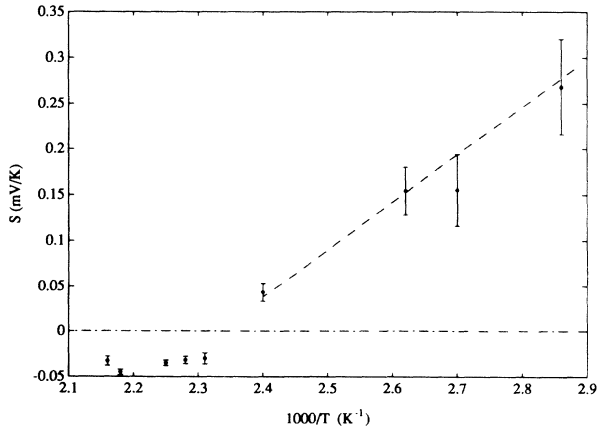

FIG. 1. Temperature dependence of thermopower in iron thiophosphate. The solid circle and the dashed line represent the experimental data and the best fit, respectively.

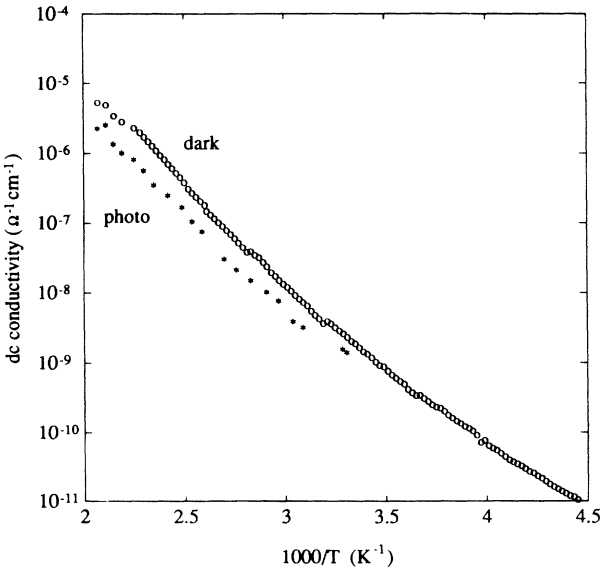

FIG. 2. Temperature dependence of the $FePS_3$ in layer dc conductivity (curve d) and photoconductivity (curve p). The latter is obtained with a visible transmitting filter.

TABLE I. Preexponential factors σ_0 and activation energies E obtained by fitting the low-temperature dark conductivity and photoconductivity experimental curves. The room-temperature conductivity σ_{RT} values are also indicated.

$FePS_3$ *p*-type	σ_{RT} ($\Omega^{-1}cm^{-1}$)	σ_0 ($\Omega^{-1}cm^{-1}$)	E (eV)
Dark conductivity (σ_d)	2.32×10^{-9}	1.67×10^{1}	0.60±0.01
Photoconductivity (σ_{ph})	1.41×10^{-9}	3.51	0.59±0.01

DISCUSSION

Model

Some one-electron band structure calculations, based on different approaches, exist.[14–16] Nevertheless, they do not agree with some experimental results (e.g., soft-x-ray and optical-absorption spectra) as discussed in a previous paper.[10] Therefore, we will adopt the simplified version of the semiempirical energy-level scheme used to describe the electronic band structure of $NiPS_3$ as a guide for interpreting our experimental results. This scheme, based on the single layer approximation and on the ionic bonding model, turned out to be adequate for interpreting the electrical transport properties[10,11] of other MPS_3 compounds ($NiPS_3$ and $MnPS_3$) and for explaining some features of soft-x-ray photoemission valence-band spectra and of below-band-gap optical-absorption spectra of $FePS_3$ itself.[17] So we have hypothesized that the $FePS_3$ electronic states arrangement is the same as that of $NiPS_3$ and $MnPS_3$, with differences only in the energy separation between the levels. Such a hypothesis is supported by the structural isomorphism of these compounds.

Figure 4 shows the proposed simplified version of the energy-level scheme for $FePS_3$. In this scheme, according to which the transition-metal atom interacts weakly with the sulfur atoms, the $(P_2S_6)^{4-}$ cluster and M^{2+} ion are treated separately. The valence bands are derived from

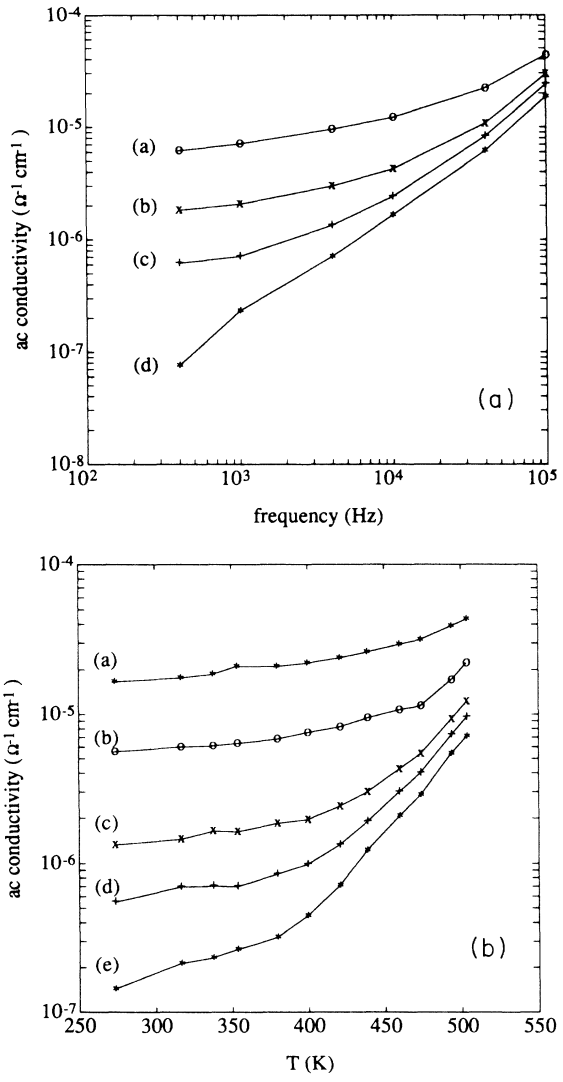

FIG. 3. (a) Frequency dependence of ac conductivity of $FePS_3$ at different temperatures: (a) 500 K; (b) 459 K; (c) 419 K; (d) 340 K. (b) Temperature dependence of ac conductivity of $FePS_3$ at different frequencies: (a) 100 kHz; (b) 40 kHz; (c) 10 kHz; (d) 4 kHz; (e) 1 kHz.

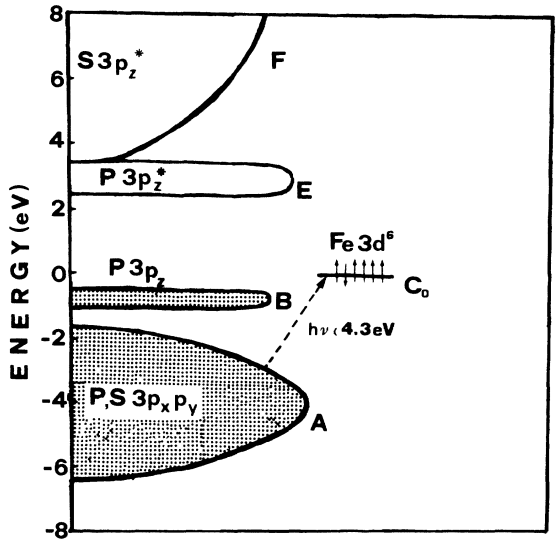

FIG. 4. Simplified version of the energy-level scheme adopted to describe the electronic band structure of $FePS_3$. A and B denote the valence bands arising from the P-S $3p_xp_y$ hybridization, and from the $3p_z$ bonding orbitals of P-P, respectively. E and F represent the lowest conduction states consisting of $3p_z^*$ antibonding orbitals of S and P. C_0 denotes the ground-state energy of the Fe^{2+} $3d$ electrons in the crystal. The energy values are referred to the Fermi energy level, which is assumed to coincide with the C_0 level (see text). In addition the light excitation process (see text) is also shown.

the P-S $3p_xp_y$ and $3s$ orbitals and from the P-P $3p_z$ bonding orbitals, which hold two PS_3 groups together on top of each other forming the octahedral-like P_2S_6 unit of the single layer. In Fig. 4 such bands are denoted by A and B, respectively. Strong hybridization between the P and S $3p_xp_y$ orbitals is suggested to account for the almost planar PS_3 groups. The antibonding P-P and S $3p_z$ orbitals empty states, which are indicated with E and F, respectively, in Fig. 4, and the M^{2+} $4s$ and $4p$ states generate the conduction bands. The M^{2+} ion $3d$ orbitals, localized on the transition-metal ion and not bonded with other orbitals, lie in the gap of the P $3p_z$ bonding-antibonding bands. The Fermi-level position coincides with that of Fe^{2+}-ion $3d$ levels, these being partially filled.

The electronic configuration and ground state of the Fe^{2+} free ion are $(3d)^6$ and ^5D, respectively. When the ligands (sulfur atoms in $FePS_3$) are placed in octahedral positions about the Fe^{2+} ion, as in the $FePS_3$ compound, the degenerate $3d$ orbitals, in which the single d electron is accommodated, split to give rise to a set of lower-energy t_{2g} orbitals and a set of higher-energy e_g orbitals. In the weak-field limit, the lowest configuration for a high-spin octahedrally coordinated Fe^{2+} complex is $(t_{2g}^4e_g^2)$, which corresponds to the ground state $^5T_{2g}$. In Fig. 4 such a state is represented by only a level, C_0, because we will not consider the d-level substructure as relevant for our discussion.

Thermopower

The thermopower measurement, in addition to that of conductivity, is a useful technique in order to identify the dominant conduction mechanism, or to decide whether two conduction processes participate in parallel.[18] Moreover, if the nature of the charge transport can be determined, information can be obtained about the nature of the electronic states in which the transport occurs. For ambipolar conduction in a crystalline nondegenerate semiconductor the thermoelectric power is given by

$$S=(S_n\sigma_n+S_p\sigma_p)/(\sigma_n+\sigma_p)\ , \tag{3}$$

where σ_n and σ_p are the contributions to conduction from electrons and holes, respectively, and S_n and S_p are,

$$S_n=-(k/e)[(E_c-E_f)/kT+a_n]\ , \tag{4}$$

$$S_p=(k/e)[(E_f-E_v)/kT+a_p]\ . \tag{5}$$

Here, E_c and E_v are the conduction-band minimum and the valence-band maximum, respectively, and a_n and a_p are constants of the order of 2–4, depending on the predominant scattering mechanism. These constants represent the transfer of kinetic energy through the sample due to the fact that the average carrier energy relative to the band edge is greater at the hot end than at the cold end. In an intrinsic semiconductor, the Fermi energy is essentially equidistant from the valence- and conduction-band edges. Thus, since S_n and S_p are nearly equal and opposite, Eq. (3) shows that the thermopower will be dominated by the carriers that have the larger mobility. Therefore, the sign of S is usually a good guide to determine whether electrons or holes dominate the conduction.

The observed variation of the $FePS_3$ thermopower with temperature can be divided in two regions. In region I (below 430 K), S is thermally activated with an activation energy E_s of (0.52 ± 0.07) eV and shows a positive sign, as reported by other researchers.[9] The fact that the magnitude of S increases with decreasing temperature means that the conduction mechanism takes place near the band edge,[19] and that $FePS_3$ behaves as a semiconductor. Besides, given that the sign of the thermopower is determined by whether the dominant conduction mechanism takes place above or below the Fermi level, which is located on the C_0 state, the positive sign of the $FePS_3$ thermopower and the obtained activation energy value suggest that the dominant conduction process is due to holes in the valence band originating from the P $3p_z$ bonding states (the B band of Fig. 4). Thus, in this temperature range, $FePS_3$ behaves as a p-type semiconductor, as do the isostructural $MnPS_3$ and $NiPS_3$ compounds.[10,11]

In addition, the relatively small Seebeck coefficient values of the order of 130 μV are typical of relatively high electrical conductivity materials.[20] In fact, $FePS_3$ shows a lower resistance value than that observed in $MnPS_3$ and $NiPS_3$.

In region II (above 430 K), the behavior of S is different from that observed in region I. In fact, as reported in Fig. 1, S decreases with increasing temperature and becomes, above 450 K, independent of temperature and negative. This is an indication that a conduction mechanism, occurring in a different energy channel, becomes predominant at the highest temperatures. In fact, the unactivated temperature behavior and the negative sign of S make it plausible to hypothesize that an electron hopping conduction mechanism is taking place at the Fe^{2+} $3d$ states. The small hole mobility value, derived in the next section from the dark-conductivity data, and the increased phonon-assisted hopping probability at the highest temperatures, support such a hypothesis.

Dark conductivity

Dark-conductivity measurements on $FePS_3$ can be approximated by a single activation energy in the same temperature range where S was thermally activated. The calculated activation energy value E_d is (0.60 ± 0.01) eV and coincides, within the estimated errors, with the value of the thermopower activation energy E_s. Such a coincidence constitutes a minimum criterion for one-carrier conductivity in extended states.[19] Thus, for temperatures below 430 K the same conduction mechanism observed in Fig. 1 for S, namely by holes in the valence P $3p_z$ band, is to be supposed. Assuming for the density of states, N_0, in the P $3p_z$ band the typical value for the parabolic band approximation, i.e., $N_0=2.51\times10^{13}$ cm^{-3}, we have also calculated the carrier mobility μ using the relation $\sigma_0=e\mu N_0$, where σ_0 is the dark-conductivity preexponential value reported in Table I. We have obtained for μ a value of 4.16 cm^2 V^{-1} s^{-1}. Such a mobility value, adequate for an extended band conduction mechanism, is

almost equal to that deduced for the $MnPS_3$ carrier mobility from analogous measurements.[11]

Above 430 K a more-detailed discussion of the conduction mechanism was not possible because data became more scattered and we were not able to extend the measurements beyond 500 K due to experimental limitations.

Photoconductivity

In $FePS_3$ the main absorption edge of 1.59 eV, observed in the optical spectra, has been assigned, on the basis of matrix element considerations, to charge-transfer transitions from the P-S orbitals to the Fe^{2+} empty $3d$ states.[17] In fact, as in $MnPS_3$ and $NiPS_3$, symmetry considerations prohibit first- and second-order transitions from P $3p_z$ band (B band in Fig. 4) to Fe^{2+} $3d^6$ levels.[10] Therefore, when $FePS_3$ is exposed to light of higher energy ($1.75\ \text{eV} < h\nu < 4.3\ \text{eV}$), generation of free holes in band A and of electrons in level C_0 results. The occupied centers in the B band behave as hole recombination centers of density n_r. Since $\sigma_{\text{ph}} \leq \sigma_d$ (low light), the density of excited carriers c is proportional to the carrier lifetime τ_c:

$$c = f\tau_c \ , \tag{6}$$

where f is the generation of free electrons and free holes volume rate and c is equal to n or to p, the equilibrium carrier densities, if the excited carrier is an electron or a hole, respectively.[21] In addition, the carrier lifetime is given by

$$\tau_c = 1/(c_r v s_c) \ , \tag{7}$$

where v, c_r, and s_c are the thermal velocity, the recombination centers density, and the capture cross section for the given free carrier, respectively.[21] Here, as in the $NiPS_3$ and $MnPS_3$ cases, since the recombination centers belong to the band B, we find that $p_r \ll n_r$, where p_r is the density of the unoccupied centers that behave as electron recombination centers. Assuming that $s_n = s_p = s$, and that the thermal velocities v of both carriers are equal, we find that $\tau_n \gg \tau_p$ and the process with the smaller associated lifetime is the one to be seen in photoconductivity. Thus the observed activation energy of about 0.59 eV represents the energy separation between A band top and B band bottom, namely between the P $3p_z$ and P-S $3p_x p_y$ bands. Moreover, using the E_g value of 1.59 eV (Ref. 17) and writing the energy gap as follows:

$$E_g = E_f - E_v = E_d + E_{\text{ph}} + \Delta E_z \tag{8}$$

we obtain for the P $3p_z$ band a bandwidth of about 0.5 eV. This value is the same as that estimated for the P $3p_z$ band of the $NiPS_3$ compound.[10] Such a coincidence, supporting the fact that the transition-metal $3d$ levels play no significant role in the P—S bonding, confirms the validity of the transition-metal weakly interacting model[12] for the interpretation of the electronic properties of these layered semiconductor compounds.

ac conductivity

Valuable information on the electrical transport mechanisms in solids can be gained by studying the temperature dependence of ac conductivity. At lower frequencies, ac-conductivity measurements can be viewed largely as an extension of the traditional dc ones. However, at higher frequencies contact effects and internal barriers become capacitively short circuited and losses are expected to reflect the bulk dissipative mechanisms. In general, ac conductivity $\sigma_{\text{ac}}(\omega)$ is found to vary with angular frequency ω as

$$\sigma_{\text{ac}} = \sigma(0) + \sigma_1 \tag{9}$$

at frequencies well below the lattice vibrational frequency.[22] In the above equation, $\sigma(0)$ is the dc limit of the conductivity and σ_1 is an additional frequency-dependent conductivity given by

$$\sigma_1 = A\omega^s \ , \tag{10}$$

where A is a temperature-dependent parameter and s is found to take values around 1.[22] Moreover, according to Mott and Davis[23] information about localized states can be obtained by studying the ac conductivity. Whereas $\sigma(0)$ is considered as being due to different transport mechanisms (band conduction, band tail, etc.), depending on the temperature range investigated, $\sigma_1 = A\omega^s$ always results from processes operating near the Fermi level.[23,24] For a wide variety of low-mobility solids the ac conductivity due to the hopping of carriers is expected to be proportional to ω^s, where $0.5 < s < 2$, whereas normal band type ac conductivity is expected to be largely frequency independent.[24] The lower value of s may occur for multiple hops while the higher value occurs for single hops.[25]

Although the ac conductivity of several crystalline solids has been extensively studied,[23,26,27] to our knowledge no such study has been reported in the literature for the $FePS_3$ compound. The $\sigma_{\text{ac}} \sim \omega^s$ dependence observed at temperatures below 400 K with $s = 0.89$ and the $FePS_3$ low-mobility value deduced from the dark-conductivity data suggest that the dominant conduction mechanism at the lower temperatures is by the hopping of charge carriers in the Fe^{2+} $3d$ levels. In an ionic material such as $FePS_3$, we may expect the $3d$ holes to be polarons[28] or carriers "dressed" by a cloud of lattice polarization. Then, thermally activated hopping of small polarons from an Fe^{2+} to an Fe^{3+} site could give rise to the observed $\sigma_{\text{ac}} \sim \omega^s$-type dependence, characteristic of carriers hopping between localized states.[23,26,27] With regard to the frequency-independent ac conductivity at higher temperatures, it may be due to multiple hops between the $3d$ localized states as the hopping process is phonon assisted.[26,27] In fact, according to Pollak,[29] at high temperatures multiple hops occur frequently while at low temperatures single hops predominate. This leads to an increased thermal activation at high temperatures with a corresponding decrease in the frequency dependence.

CONCLUSIONS

From the analysis of the transport properties of the layered semiconductor $FePS_3$ several conclusions can be drawn.

(i) The thermopower measurements locate the P $3p_z$ band about 0.52 eV lower than the partially filled Fe^{2+} $3d$ levels and suggest a p-type semiconduction at temperatures below 430 K and a hopping of electrons between Fe^{2+} $3d$ localized states at higher temperatures.

(ii) The activation energy value, obtained from the photoconductivity data, gives the energy separation between the P $3p_z$ and P-S $3p_xp_y$ valence bands.

(iii) The resulting $FePS_3$ P $3p_z$ bandwidth value agrees well with that obtained for $NiPS_3$.

(iv) The observed frequency-dependent conductivity can be described by a thermally activated hopping of small polarons from an Fe^{2+} to an Fe^{3+} site, while the frequency-independent ac conductivity at higher temperatures may be due to multiple hops between the $3d$ localized states.

All the above features support the hypothesis that the transition-metal weakly interacting model[12] is adequate for interpreting most of the electronic properties of this material, as in the $NiPS_3$ and $MnPS_3$ cases.

[1]A. Le Mehaute, G. Ouvrard, R. Brec, and J. Rouxel, Mater. Res. Bull. **12**, 1191 (1977).

[2]A. H. Thompson and M. S. Whittingham, Mater. Res. Bull. **12**, 741 (1977).

[3]R. Brec, D. Schleich, A. Louisy, and J. Rouxel, Ann. Chim. Fr. **3**, 347 (1978).

[4]J. Rouxel, P. Molinie, and L. H. Top, J. Power Sources **9**, 345 (1983).

[5]K. Okuda, K. Kurosawa, and S. Saito, in *High Field Magnetism*, edited by M. Date (North-Holland, Amsterdam, 1983), p. 55.

[6]K. Kurosawa, S. Saito, and Y. Yamaguchi, J. Phys. Soc. Jpn. **52**, 3919 (1983).

[7]G. Ouvrard, Ph.D. thesis, University of Nantes, 1980.

[8]R. Brec, Solid State Ion. **22**, 3 (1986).

[9]P. J. S. Foot, J. Suradi, and P. A. Lee, Mater. Res. Bull. **15**, 189 (1980).

[10]V. Grasso, F. Neri, S. Santangelo, L. Silipigni, and M. Piacentini, Phys. Rev. B **37**, 4419 (1988).

[11]V. Grasso, F. Neri, S. Santangelo, L. Silipigni, and M. Piacentini, J. Phys. Condens. Matter **1**, 3337 (1989).

[12]M. Piacentini, F. S. Kumalo, C. G. Olson, J. W. Anderegg, and D. W. Lynch, Chem. Phys. **65**, 289 (1982).

[13]K. S. Krane and L. Schecter, Am. J. Phys. **50**, 1 (1982).

[14]M. H. Whangbo, R. Brec, G. Ouvrard, and J. Rouxel, Inorg. Chem. **24**, 2459 (1985).

[15]H. Mercier, Ph.D. thesis, University of Nantes, 1985, p. 48.

[16]N. Kurita and K. Nakao, J. Phys. Soc. Jpn. **58**, 610 (1989).

[17]M. Piacentini, F. S. Kumalo, G. Leveque, C. G. Olson, and D. W. Lynch, Chem. Phys. **72**, 61 (1982).

[18]*Treatise on Solid State Chemistry*, Vol. 2 of *Defects in Solids*, edited by N. B. Hannay (Plenum, New York, 1975), Chap. 4.

[19]H. A. Vander Plas and R. H. Bube, J. Non-Cryst. Solids **24**, 377 (1977).

[20]W. Waclawek and M. Zabkowska, J. Phys. E **14**, 618 (1981).

[21]A. Rose, *Concepts in Photoconductivity and Allied Problems* (Krieger, New York, 1978), Chap. 3.

[22]A. K. Jonscher, Nature **267**, 673 (1977).

[23]N. F. Mott and E. A. Davis, *Electronic Processes in Non-Crystalline Materials* (Oxford University Press, London, 1971).

[24]E. A. Davis and N. F. Mott, Philos. Mag. **22**, 903 (1970).

[25]M. Pollak and T. H. Geballe, Phys. Rev. **122**, 1742 (1961).

[26]A. I. Lakatos and M. Abkowitz, Phys. Rev. B **3**, 1791 (1971).

[27]M. Abkowitz, A. Lakatos, and H. Scher, Phys. Rev. B **9**, 1813 (1974).

[28]J. Yamashita and T. Kurosawa, J. Phys. Chem. Solids **5**, 34 (1958).

[29]M. Pollak, Phys. Rev. **138**, A1822 (1965).

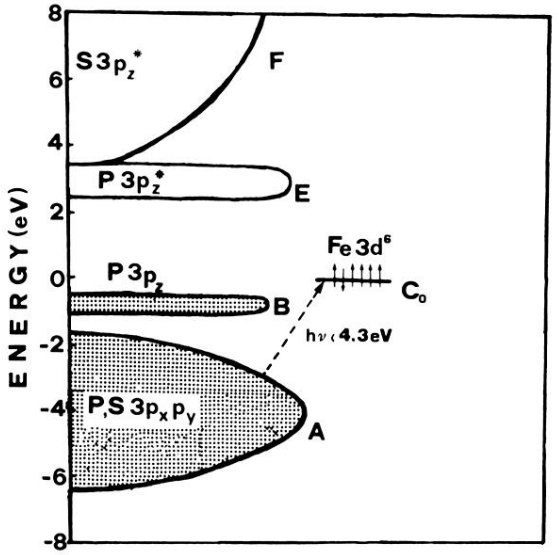

FIG. 4. Simplified version of the energy-level scheme adopted to describe the electronic band structure of $FePS_3$. A and B denote the valence bands arising from the P-S $3p_xp_y$ hybridization, and from the $3p_z$ bonding orbitals of P-P, respectively. E and F represent the lowest conduction states consisting of $3p_z^*$ antibonding orbitals of S and P. C_0 denotes the ground-state energy of the Fe^{2+} $3d$ electrons in the crystal. The energy values are referred to the Fermi energy level, which is assumed to coincide with the C_0 level (see text). In addition the light excitation process (see text) is also shown.